

# Sandbar-Shoreline coupling on an embayed beach



Universiteit Utrecht

Wietse van de Lageweg<sup>1</sup>, Karin Bryan<sup>2</sup>, Giovanni Coco<sup>3</sup> and Gerben Ruessink<sup>1</sup>

1) Utrecht University, The Netherlands, 2) University of Waikato, New Zealand, 3) NIWA, New Zealand

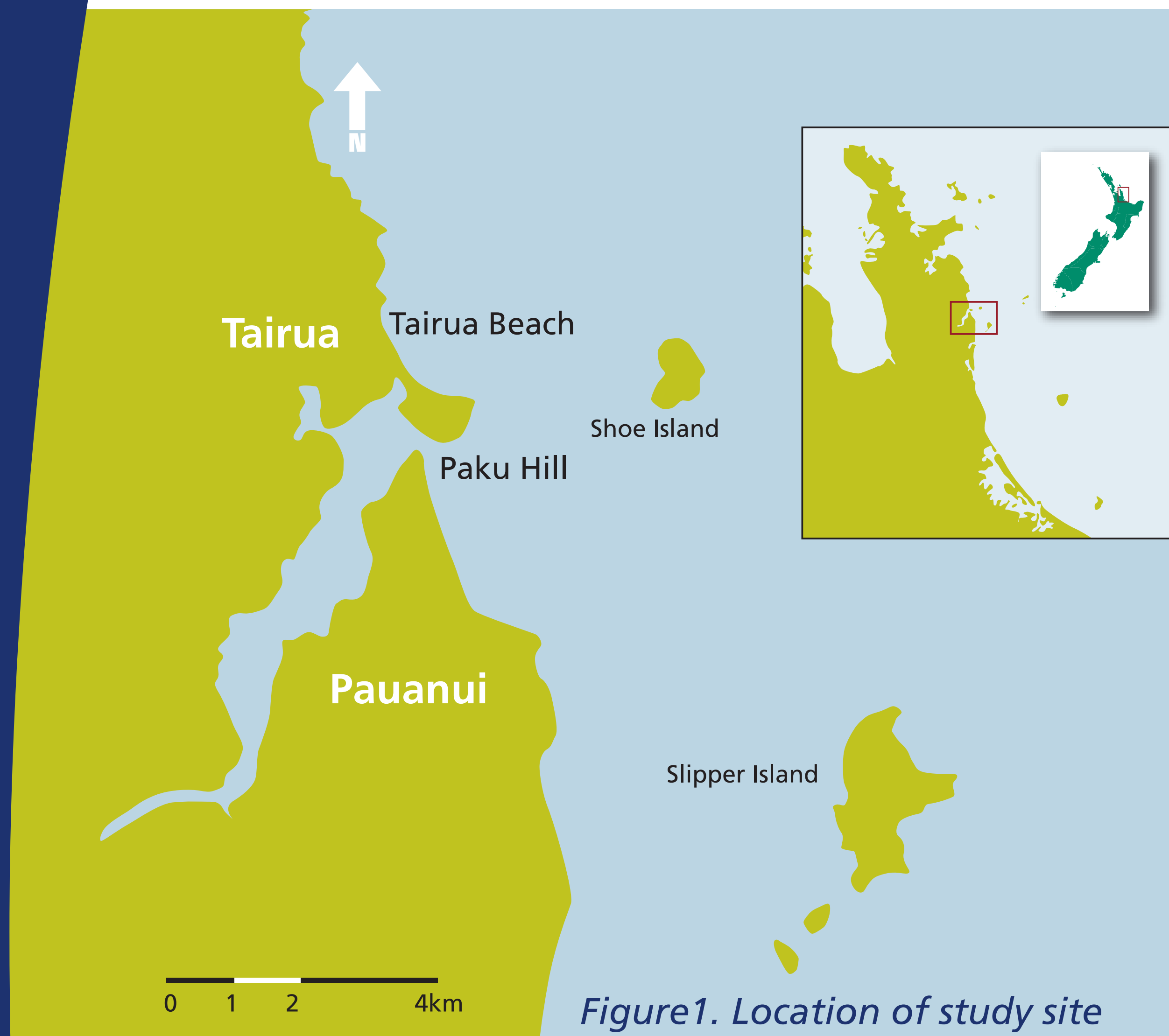


Figure 1. Location of study site

## Introduction

Alongshore rhythmic shoreline patterns are often coupled to rhythmic (crescentic) sandbar patterns. Quantitative observations are, however, limited. The aims of our study were (1) to analyze the spatial and temporal behaviour of medium-scale nearshore morphology, and (2) to explore the conditions, spatial and temporal scales and variability involved in the coupling between shoreline and sandbar patterns.

## Methods

We used a 7-year data set of daily shoreline and sandbar observations collected at the embayed Tairua Beach in New Zealand (Figure 1). The beach is characterised by the presence of crescentic sandbar patterns and well-developed rips. The shoreline and sandbar data set were extracted from video images collected at Tairua by the NIWA (Figure 2).



Figure 2. Applied video imagery technique showing Cam-era time-exposure image.

## Results

Changes in morphodynamic state are dominantly triggered by storm events (Figure 3). For the first three years a strong coupling between shoreline and sandbar exists during summer periods, while they are only weakly coupled or decoupled during winter periods (Figures 5 and 6).

Figure 3. Time stacks showing rotation lines for (A) the shoreline and (B) the sandbar. Time series of the alongshore component of the ten-day-averaged wave energy  $E_x$  are indicated in (a) and (b). The rotation lines are horizontally stacked with warm (cold) colours indicating seaward (landward) oscillations.

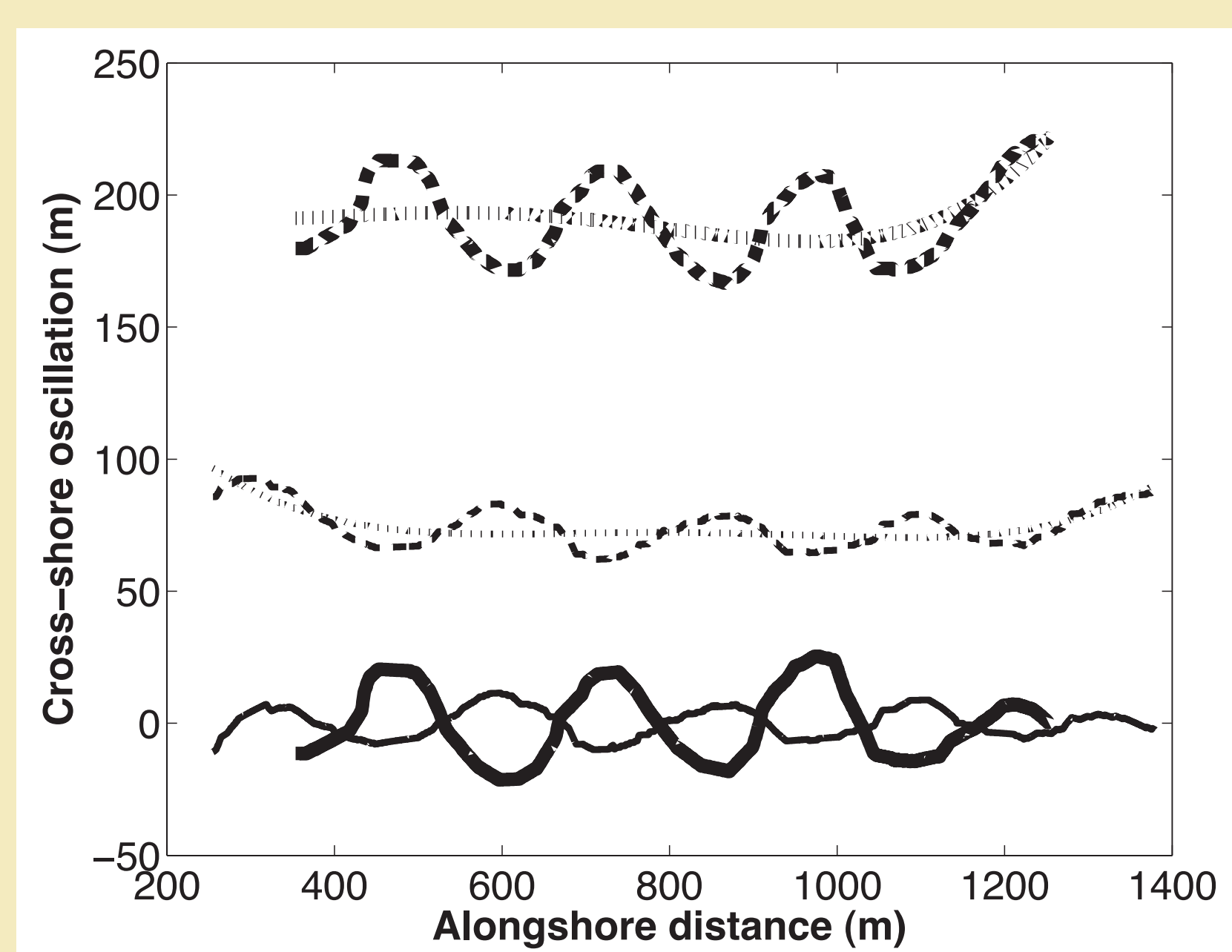
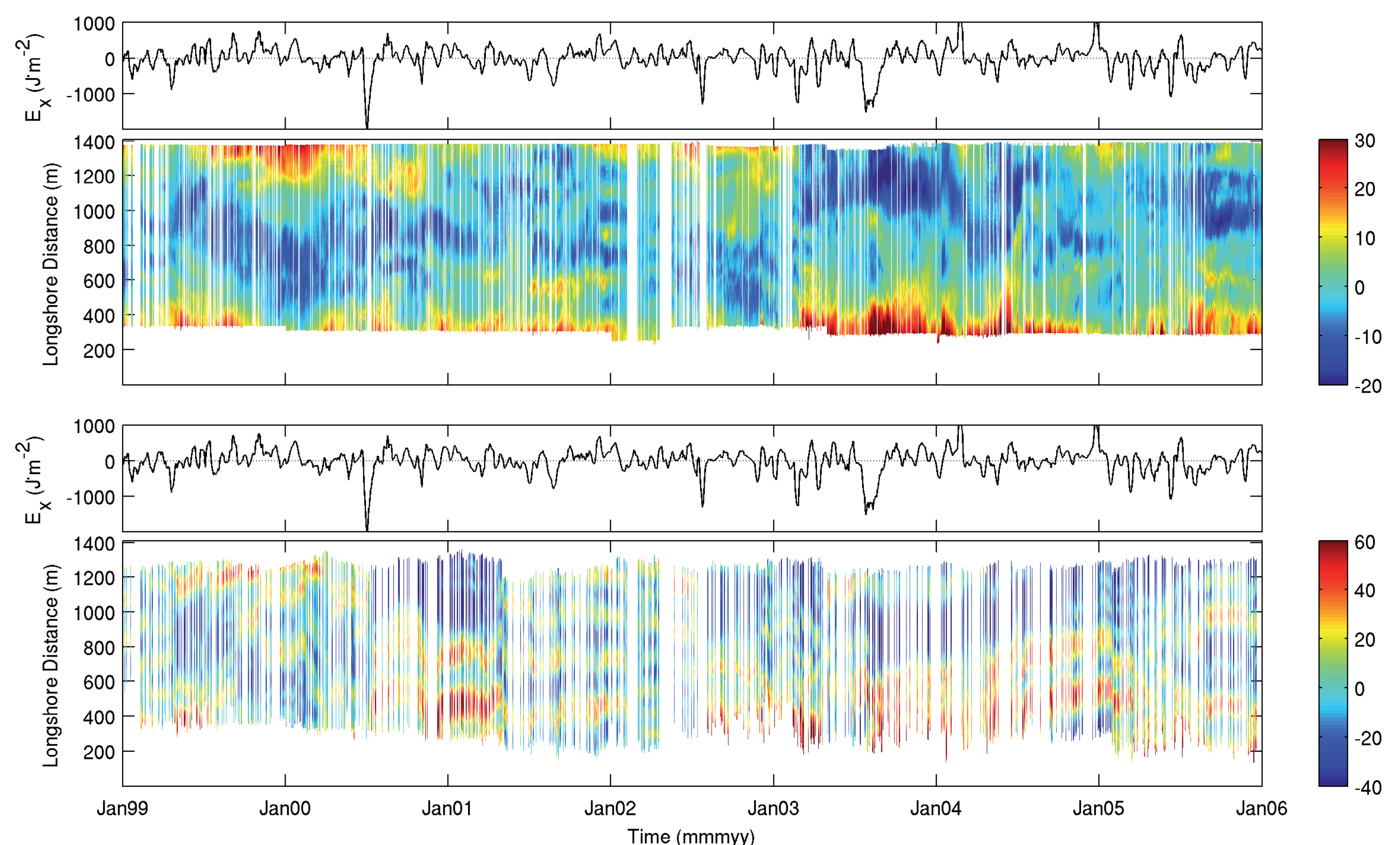


Figure 4. Observed example configuration of a high negative ( $r = -0.85$ ) correlation. Dashed lines are the detected bar (thick) and shoreline, the dotted lines are 4<sup>th</sup> order polynomial fits of these configurations and the solid lines represent the subtraction of the polynomial fit of the detected bar and shoreline. Correlations are evaluated on this latter configuration.

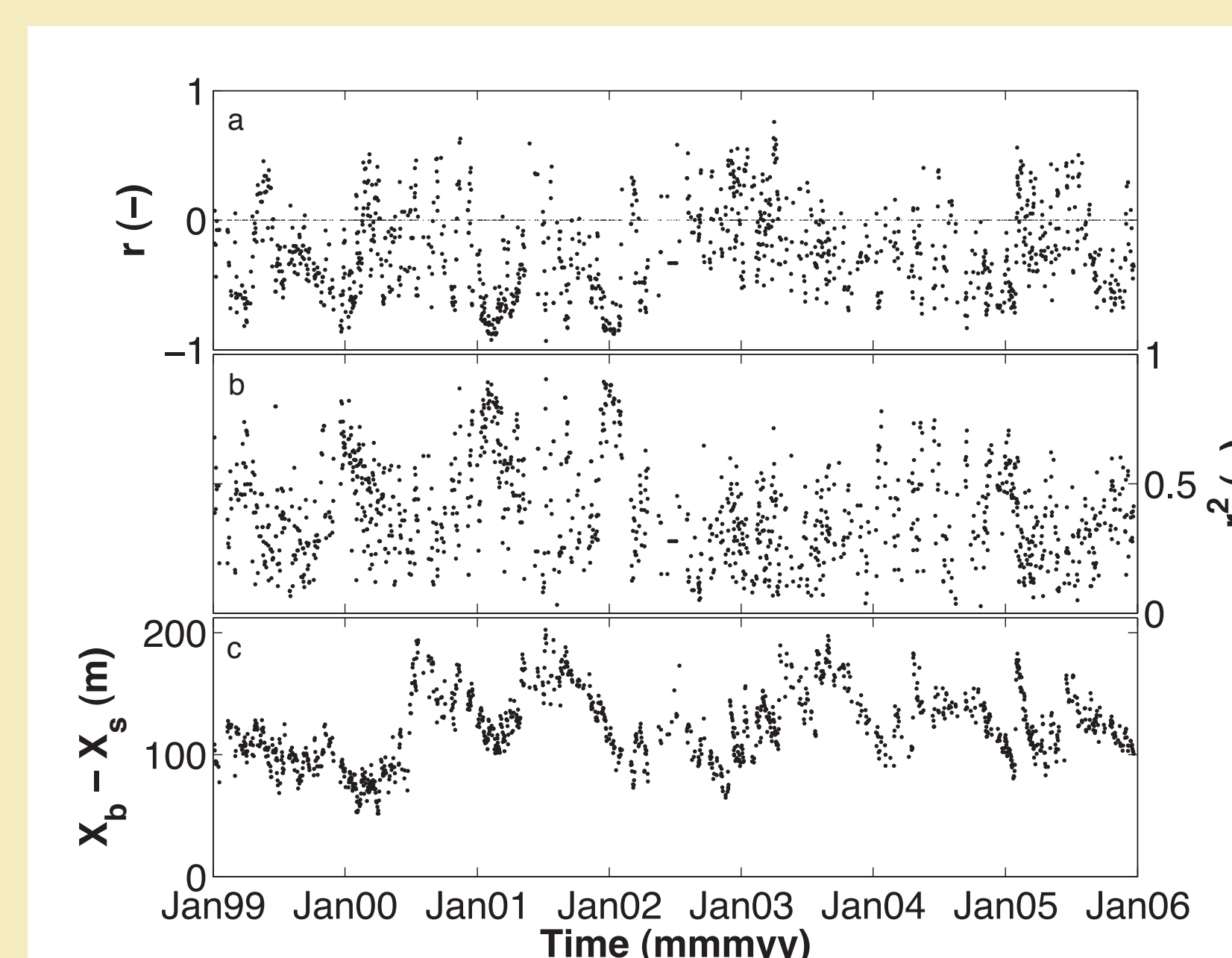


Figure 5. Time series of (a) the 4<sup>th</sup> order polynomial bar and shoreline correlation ( $r$ ) at zero spatial lag, (b) the maximum 4<sup>th</sup> order polynomial bar and shoreline cross-correlation ( $r^2$ ) by shifting the spatial domain from lag -200 m to +200 m, and (c) the distance between the alongshore mean shoreline and sandbar.

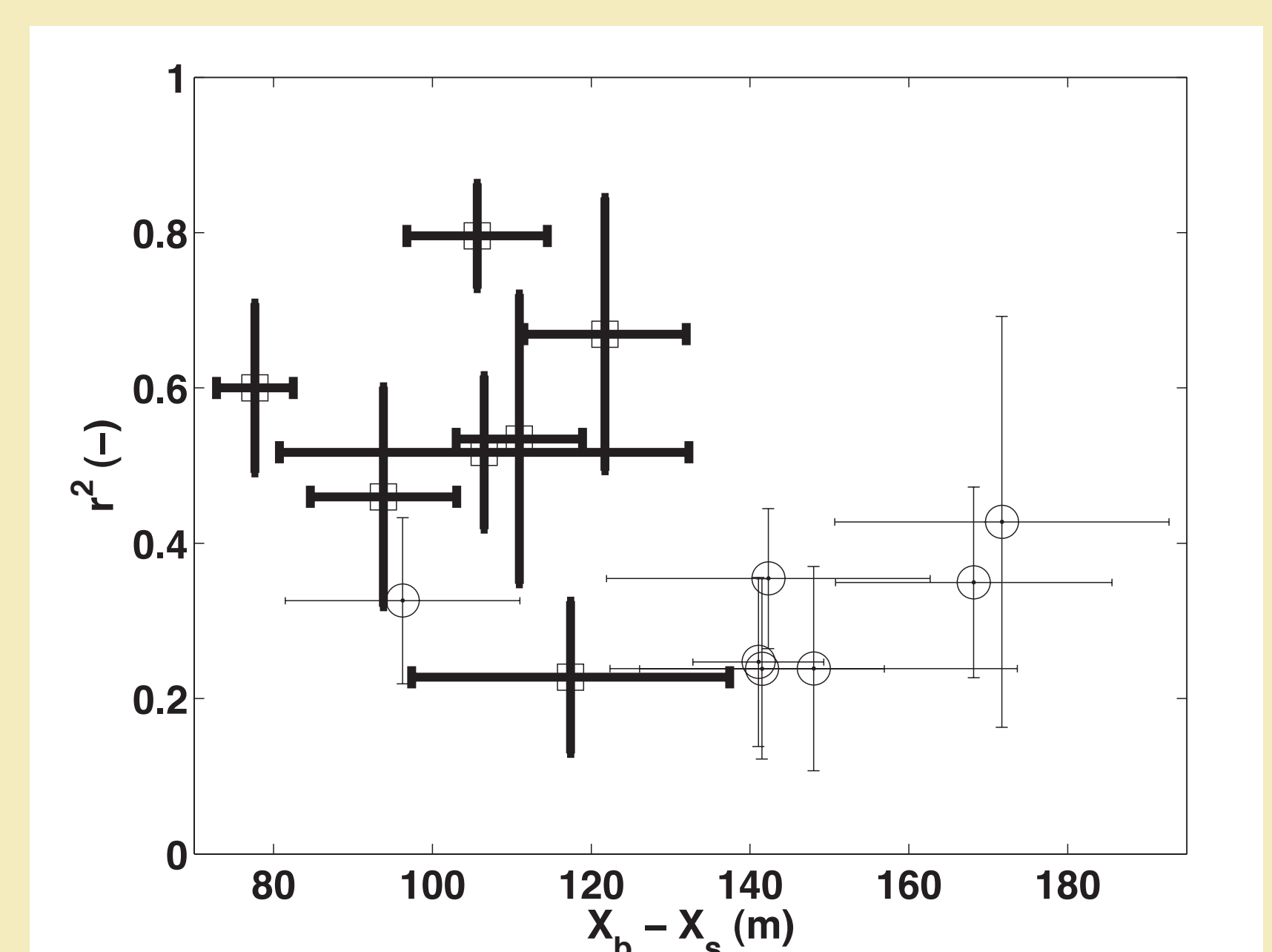


Figure 6. Average seasonal cross-correlation ( $r^2$ ) as a function of the average seasonal distance between sandbar and shoreline. Squares (circles) are average values and thick (thin) error bars indicate standard deviations for the summer (winter) season.